Diet-Induced Muscle Insulin Resistance Is Associated With Extracellular Matrix Remodeling and Interaction With Integrin $\alpha_2\beta_1$ in Mice

Li Kang,[1] Julio E. Ayala,[1,2] Robert S. Lee-Young,[1] Zhonghua Zhang,[3] Freyja D. James,[1] P. Darrell Neufer,[4] Ambra Pozzi,[5] Mary M. Zutter,[3] and David H. Wasserman[1,2]

OBJECTIVE—The hypothesis that high-fat (HF) feeding causes skeletal muscle extracellular matrix (ECM) remodeling in C57BL/6J mice and that this remodeling contributes to diet-induced muscle insulin resistance (IR) through the collagen receptor integrin $\alpha_2\beta_1$ was tested.

RESEARCH DESIGN AND METHODS—The association between IR and ECM remodeling was studied in mice fed chow or HF diet. Specific genetic and pharmacological murine models were used to study effects of HF feeding on ECM in the absence of IR. The role of ECM-integrin interaction in IR was studied using hyperinsulinemic-euglycemic clamps on integrin $\alpha_2\beta_1$-null (*itga2*$^{-/-}$), integrin $\alpha_1\beta_1$-null (*itga1*$^{-/-}$), and wild-type littermate mice fed chow or HF. Integrin $\alpha_2\beta_1$ and integrin $\alpha_1\beta_1$ signaling pathways have opposing actions.

RESULTS—HF-fed mice had IR and increased muscle collagen (Col) III and ColIV protein; the former was associated with increased transcript, whereas the latter was associated with reduced matrix metalloproteinase 9 activity. Rescue of muscle IR by genetic muscle-specific mitochondria-targeted catalase overexpression or by the phosphodiesterase 5a inhibitor, sildenafil, reversed HF feeding effects on ECM remodeling and increased muscle vascularity. Collagen remained elevated in HF-fed *itga2*$^{-/-}$ mice. Nevertheless, muscle insulin action and vascularity were increased. Muscle IR in HF-fed *itga1*$^{-/-}$ mice was unchanged. Insulin sensitivity in chow-fed *itga1*$^{-/-}$ and *itga2*$^{-/-}$ mice was not different from wild-type littermates.

CONCLUSIONS—ECM collagen expansion is tightly associated with muscle IR. Studies with *itga2*$^{-/-}$ mice provide mechanistic insight for this association by showing that the link between muscle IR and increased collagen can be uncoupled by the absence of collagen-integrin $\alpha_2\beta_1$ interaction. ***Diabetes*** **60:416–426, 2011**

The inflammatory response associated with insulin resistance may have extensive effects on extracellular matrix (ECM) remodeling and endothelial cell function. ECM adaptations that accompany insulin resistance in muscle are of great potential significance. Collagens, the most abundant structural components of ECM, not only support tissues but are also required for cell adhesion and migration during growth, differentiation, morphogenesis, and wound healing (1). Over 90% of the collagens expressed in skeletal muscle are composed of collagen (Col) I, III, and IV. Although ColI and ColIII comprise the fibrillar-type collagen (1), ColIV is the most abundant structural component of the basement membrane (2,3). Seminal studies have shown that insulin resistant human skeletal muscle is characterized by increased collagen (4,5). However, the functional connection between insulin resistance and ECM expansion has received little attention. Moreover, the mechanism(s) of changes in collagens with insulin resistance is poorly defined.

Integrins are cell surface receptors that interact with ECM and mediate both inside-out and outside-in signaling (6,7). Of the 24 integrins identified in mammals, only four of them bind collagens. These four collagen receptor integrins share the β_1-subunit, which heterodimerizes with either the α_1-, α_2-, α_{10}-, or α_{11}-subunit (8). Previous studies showed that activation of focal adhesion kinase, which is downstream of integrin activation, was decreased in insulin resistant skeletal muscle of high fat (HF)-fed rats (9). Moreover, mice lacking integrin β_1 expression specifically in striated muscle develop insulin resistance (10). These data suggest a role for collagen-integrin interaction in the development of insulin resistance.

The two major collagen binding receptors, integrins $\alpha_1\beta_1$ and $\alpha_2\beta_1$, are structurally similar but activate distinct signaling pathways (11,12). Integrin $\alpha_1\beta_1$ is antifibrotic since integrin α1-null mesangial cells show increased reactive oxygen species (ROS) production and collagen synthesis (13,14). In contrast, integrin $\alpha_2\beta_1$ is profibrotic since activation of integrin $\alpha_2\beta_1$ leads to increased ROS production (15) and collagen expression (16,17). Integrins $\alpha_1\beta_1$ and $\alpha_2\beta_1$ are both expressed on endothelial cells but have opposing effects on endothelial cell biology. Integrin $\alpha_1\beta_1$ is proangiogenic, and its deletion leads to decreased endothelial cell proliferation and angiogenesis in vivo (18,19). In contrast, integrin $\alpha_2\beta_1$ is antiangiogenic and its deletion results in increased endothelial cell proliferation and angiogenesis in vivo (20).

Herein we tested the hypothesis that the inflammatory response associated with HF diet-induced insulin resistance increases collagen in skeletal muscle of the mouse and that this increase contributes to insulin resistance by collagen receptor integrins $\alpha_1\beta_1$ and $\alpha_2\beta_1$. The specific goals were to determine in HF-fed C57BL/6J mice whether *1*) collagen accumulation in muscle occurs and the mechanisms for any accumulation; *2*) a pharmacological or genetic manipulation that corrects muscle insulin

From the [1]Department of Molecular Physiology and Biophysics, Vanderbilt University, Nashville, Tennessee; the [2]Mouse Metabolic Phenotyping Center, Vanderbilt University, Nashville, Tennessee; the [3]Department of Pathology, Vanderbilt University, Nashville, Tennessee; the [4]Department of Exercise and Sport Science & Physiology, East Carolina University, Greenville, North Carolina; and the [5]Nephrology Division, Vanderbilt University, Nashville, Tennessee.

Corresponding author: Li Kang, li.kang@vanderbilt.edu.

Received 6 August 2010 and accepted 10 November 2010.

DOI: 10.2337/db10-1116

This article contains Supplementary Data online at http://diabetes.diabetesjournals.org/lookup/suppl/doi:10.2337/db10-1116/-/DC1.

resistance of HF feeding eliminates collagen accumulation and increases muscle vascularization; and *3*) a genetic deletion of integrin $\alpha_2\beta_1$ protects against insulin resistance and increases muscle vascularization, and a deletion of integrin $\alpha_1\beta_1$, which has actions that oppose integrin $\alpha_2\beta_1$, exacerbates insulin resistance.

RESEARCH DESIGN AND METHODS

Murine models. Mice were housed under temperature- and humidity-controlled environment with a 12-h light/dark cycle. Distinctive murine models were used to address specific goals of the study: *1*) the association between insulin resistance and ECM adaptations was studied in sex-matched C57BL/6J mice fed chow or HF diet (F3282, BioServ) containing 60% calories as fat for 20 weeks; *2*) novel genetic (muscle-specific mitochondrial-targeted catalase transgenic, $mcat^{Tg}$) and pharmacological (sildenafil) models were used to alleviate insulin resistance in the presence of HF feeding, and the rescue of the ECM adaptations was assessed; and *3*) integrin $\alpha_1\beta_1$-null ($itga1^{-/-}$) and $\alpha_2\beta_1$-null ($itga2^{-/-}$) mice were used to study the role of ECM-integrin interaction in insulin resistance.

We previously showed that $mcat^{Tg}$ mice maintained on a HF diet for 16 weeks were protected from insulin resistance (21). HF-fed mice treated with subcutaneous injection of sildenafil, a selective phosphodiesterase (PDE)5a inhibitor, for 13 weeks are also protected from insulin resistance (22). The $mcat^{Tg}$ and sildenafil-treated mice were selected as models that prevent diet-induced muscle insulin resistance based on two considerations. First, these approaches protect from diet-induced insulin resistance through specific actions that target distinct mechanisms. The $mcat^{Tg}$ mice selectively overexpress catalase in muscle mitochondria. It is a genetically modified animal model in which the rescue of diet-induced muscle insulin resistance is related to a reduction of mitochondrial release of ROS. This contrasts with the PDE5a inhibition model, which causes smooth muscle relaxation and vasodilation pharmacologically. The second consideration was that ROS have been implicated in the regulation of collagen synthesis (13,23,24), and they do so by increasing the inflammatory response and activation of mitogen-activated protein kinase (MAPK) (25,26). Therefore, $mcat^{Tg}$ mice provide a model for studying the hypothesis that the inflammatory response associated with insulin resistance increases collagen in muscle.

To further study the role of ECM-integrin interaction in insulin resistance, mice lacking the two major collagen binding receptor integrins $\alpha_1\beta_1$ or $\alpha_2\beta_1$ were studied. Male $itga2^{-/-}$ mice and wild-type (WT) littermates ($itga2^{+/+}$) were chow-fed until 9 weeks of age at which time mice were continued on chow or switched to HF diet until 23 weeks of age. Male $itga1^{-/-}$ mice and WT littermates ($itga1^{+/+}$) were chow-fed until 12 weeks of age at which time mice were continued on chow or switched to HF diet until 28 weeks of age. Murine body composition was determined by nuclear magnetic resonance. The Vanderbilt Animal Care and Use Committee approved animal procedures.

Hyperinsulinemic-euglycemic clamp (insulin clamp). Catheters were implanted in a carotid artery and a jugular vein of mice for sampling and infusions 5 days before study (27). Insulin clamps were performed on 5-h fasted mice (28). [3-^{3}H]glucose was primed (2.4 μCi) and continuously infused for a 90-min equilibration period (0.04 μCi/min) and a 2-h clamp period (0.12 μCi/min). Baseline blood or plasma parameters were determined in blood samples collected at −15 and −5 min. At t = 0, insulin infusion (4 mU/kg/min) was started and continued for 165 min. Blood glucose was clamped at 150 ~160 mg/dL using a variable rate of glucose infusion (GIR). Mice received heparinized saline-washed erythrocytes from donors at 5 μL/min to prevent a fall of hematocrit. Insulin clamps were validated by assessment of blood glucose over time. Blood glucose was monitored every 10 min, and the GIR was adjusted as needed. Blood was taken at 80–120 min for the determination of [3-^{3}H]glucose. Clamp insulin was determined at t = 100 and 120 min. At 120 min, 13 μCi of 2[^{14}C]deoxyglucose ([^{14}C]2DG) was administered as an intravenous bolus. Blood was taken at 2–35 min for the determination of [^{14}C]2DG. After the last sample, mice were anesthetized and tissues were collected.

Insulin clamp plasma and tissue sample processing. Plasma insulin was determined by ELISA (Millipore). Radioactivity of [3-^{3}H]glucose, [^{14}C]2DG, and [^{14}C]2DG-6-phosphate were determined by liquid scintillation counting (22). Glucose appearance (R_a) and disappearance (R_d) rates were determined using non-steady-state equations (29). Endogenous glucose production (endoR_a) was determined by subtracting the GIR from total R_a. The glucose metabolic index (R_g) was calculated as previously described (30).

Immunohistochemistry. ColI, ColIII, ColIV, and Von Willebrand factor (VWF) were assessed by immunohistochemistry in paraffin-embedded tissue sections. Sections (5 μm) were incubated with the following primary antibodies for 60 min: anti-ColI (Abcam), anti-ColIII (CosmoBio), anti-ColIV (Abcam), or anti-VWF (DakoCytomation). Slides were lightly counterstained with Mayer hematoxylin. The EnVision+HRP/DAB System (DakoCytomation) was used to produce localized, visible staining. Immunostaining of CD31 was performed in either frozen sections or paraffin-embedded sections using anti-CD31 (BD Biosciences). Images were captured using a Q-Imaging Micropublisher camera mounted on an Olympus upright microscope. Immunostaining was quantified by ImageJ or BIOQUANT Life Science 2009. ColI, ColIII, and ColIV protein were measured by the integrated intensity of staining. Muscle vascularity was determined by counting CD31-positive structures and by measuring areas of VWF-positive structures.

Real-time PCRs. Total RNA was isolated from gastrocnemius using the RNeasy Fibrous Tissue Kit (Qiagen). Total RNA (1 μg) was reverse transcribed using the iScript cDNA Synthesis Kit (Bio-Rad). Real-time PCR was then performed using the SYBR Green JumpStart Taq Readymix (Sigma) on an IQ5 Multicolor Real-Time PCR Detection System (Bio-Rad). The primers used are listed in Supplementary Table 1. Data were analyzed by the $2^{-\Delta\Delta Ct}$ method (31).

Gelatin zymography. Gelatin zymography was performed to measure the activities of type IV collagenase-matrix metalloproteinase (MMP)2 and MMP9 (32). Gastrocnemius was homogenized in buffer containing 0.5% Triton X-100, 100 mM Tris-HCl, 10 mM EDTA, and 10 μL/mL protease inhibitor (pH 7.5). Homogenates were centrifuged at 13,000 rpm for 20 min at 4°C. The supernatant (500 μg) was incubated at 4°C for 2 h with 40 μL of gelatin-Sepharose (Pharmacia). After the incubation, the gelatin-Sepharose beads were resuspended in nonreducing SDS-sample buffer and loaded on 10% zymogram gels (Invitrogen). The gel was developed according to the manufacturer's instructions. Conditioned medium from HT-1080 cells was used as positive control.

Western blotting. Gastrocnemius was homogenized in buffer containing 50 mM Tris-HCl, pH 7.5, 1 mM EDTA, 1 mM EGTA, 10% glycerol, 1% Triton X-100, 1 mM DTT, 1 mM PMSF, 5 μg/mL protease inhibitor, 50 mM NaF, and 5 mM sodium pyrophosphate and centrifuged at 13,000 rpm for 20 min at 4°C. The supernatant (40 μg) was applied to 4–12% SDS-PAGE gel. Phosphorylated and total Akt/protein kinase B (PKB) were probed using phospho-Akt(Ser473) and Akt antibodies (Cell Signaling). Phosphorylated and total insulin receptor substrate-1 (IRS-1) were probed using phospho–IRS-1 (Tyr612) and IRS-1 antibodies (Upstate).

Statistical analysis. Data are expressed as means ± SE. Statistical analyses were performed using Student t test or two-way ANOVA followed by Turkey post hoc tests as appropriate. The significance level was $P < 0.05$.

RESULTS

Diet-induced insulin resistance increases skeletal muscle collagen expression. Twenty weeks of HF diet in C57BL/6J mice, a regimen that induces insulin resistance (33), caused inflammation in muscle, as gene expression of F4/80, a macrophage marker, and TNF-α, a cytokine involved in systemic inflammation, was increased in muscle of HF-fed mice compared with chow-fed mice (Fig. 2*A* and *B*). To test the hypothesis that the inflammatory response associated with diet-induced insulin resistance in mice is accompanied by increased muscle collagen, we measured collagen expression in HF-fed murine muscle. Muscle ColIII and ColIV protein were increased in HF-fed mice compared with chow-fed mice (Fig. 1*A*), but protein expression of ColI was very low and differences were undetectable.

Increases in collagen could be because of either increased synthesis or decreased degradation via MMPs. mRNA of specific collagen chains were used to assess collagen synthesis. HF feeding increased muscle mRNA of ColIα1, ColIα2, and ColIIIα1 chains, whereas mRNA of ColIV was unchanged (Fig. 1*B*). To test whether increased ColIV protein was due to reduced degradation, the activities of type IV collagenases, MMP2 and MMP9, were measured. HF feeding decreased MMP9 activity, without affecting pro-MMP2 and MMP2 activities in muscle (Fig. 1*C*).

Genetic and pharmacological rescue of skeletal muscle insulin resistance after HF feeding decreases muscle inflammation and collagen expression and improves muscle vascularization. Muscle insulin resistance was absent in HF-fed $mcat^{Tg}$ (21) and sildenafil-treated mice (22). In line with decreased muscle insulin

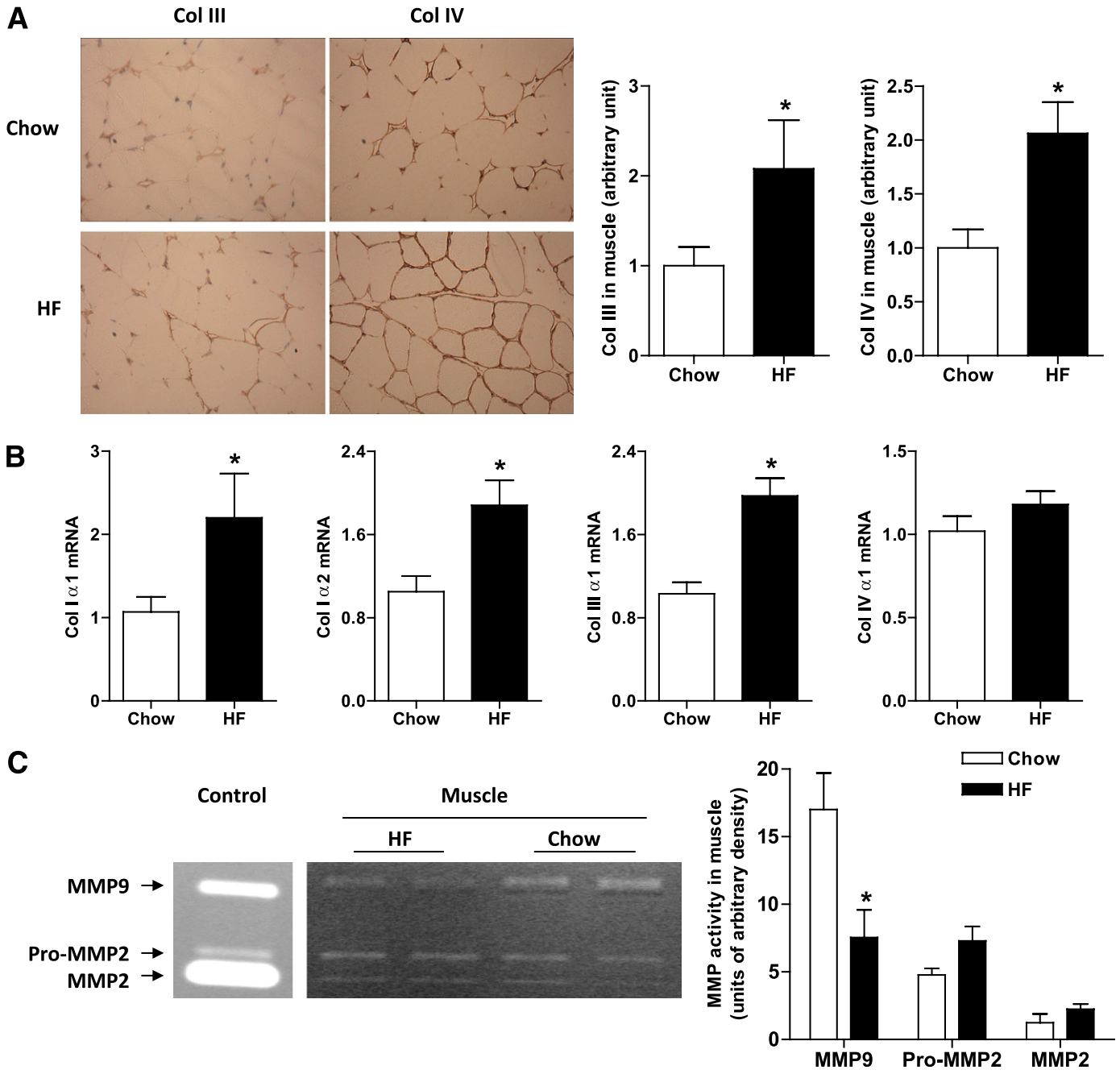

FIG. 1. HF feeding to C57BL/6J mice increased muscle collagen expression. *A*: Immunohistochemical detection of ColIII and ColIV proteins in gastrocnemius of chow-fed and HF-fed C57BL/6J mice. The magnification of images was 20×. *B*: mRNA levels of ColIα1, ColIα2, ColIIIα1, and ColIVα1. *C*: Gelatin zymogram of protein extracts from gastrocnemius of mice after either chow or HF feeding for 20 weeks. The white bands indicate the presence of type IV collagenase activity, MMP-9, pro-MMP2, and MMP2. Data are represented as means ± SE; $n = 4 \sim 7$. *$P < 0.05$ chow vs. HF. (A high-quality color representation of this figure is available in the online issue.)

resistance, both $mcat^{Tg}$ and sildenafil-treated mice had reduced F4/80 expression in muscle (Fig. 2*A* and *C*). HF diet-induced increase in muscle TNF-α mRNA was also eliminated in $mcat^{Tg}$ mice (Fig. 2*B*); although, the decrease in TNF-α mRNA in muscle of sildenafil-treated mice was nearly 50%, the measurements in WT were variable and differences were not significant (Fig. 2*D*). ColIII and ColIV proteins were decreased in $mcat^{Tg}$ and sildenafil-treated mice (Fig. 2*E*). The lower expression of ColIII in HF-fed $mcat^{Tg}$ mice was because of reduced synthesis, as the HF-induced increases in mRNA of ColIIIα1 were abolished (Fig. 3*B*). HF-induced increase in mRNA of ColIα2 was also abolished in $mcat^{Tg}$ mice (Fig. 3*A*). Decreased ColIV protein was due at least in part to increased degradation via MMP9 as MMP9 activity was increased in muscle of HF-fed $mcat^{Tg}$ and sildenafil-treated mice (Fig. 3*C*).

Decreased collagen deposition in HF-fed $mcat^{Tg}$ and sildenafil-treated mice was associated with improved muscle vascularization, since blood vessel staining by CD31 and VWF was increased (Fig. 3*D*). Taken together, preventing diet-induced muscle insulin resistance using different approaches that focus on distinct targets results in common ECM adaptations. These common adaptations

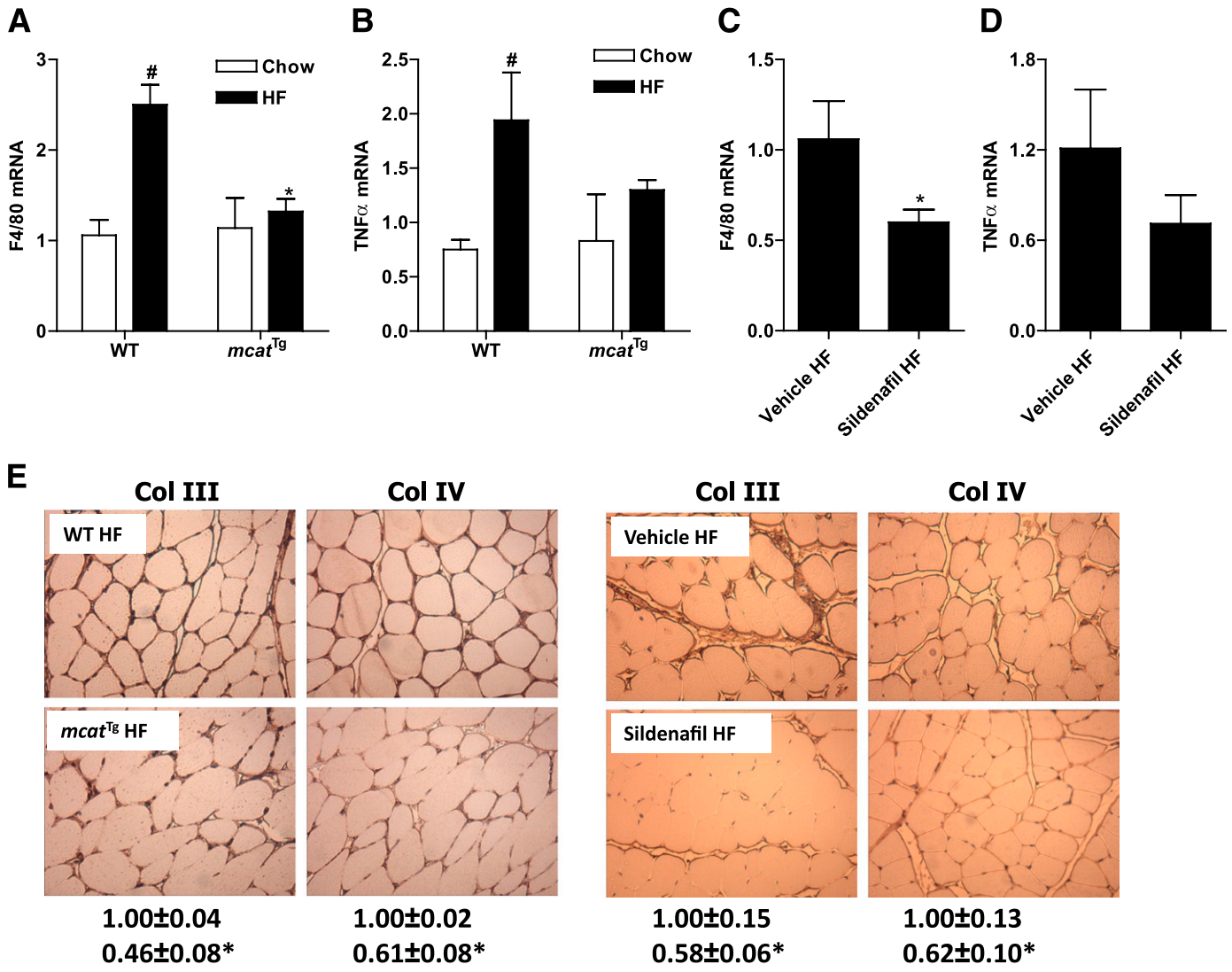

FIG. 2. Rescue of muscle inflammation and collagen expansion by catalase overexpression and chronic treatment with sildenafil. *A–D*: Muscle inflammation was assessed by measuring the mRNA levels of F4/80 and TNF-α using the quantitative real-time PCR. *E*: Immunohistochemical detection of ColIII and ColIV proteins in gastrocnemius of mice. The magnification of images was 20×. Values represent means ± SE of integrated intensity of staining for ColIII and ColIV. Data are normalized to WT HF or vehicle HF, and *n* is equal to 4 for the WT and *mcat*^{Tg} mice, 6 ~8 for the vehicle- and sildenafil-treated mice. #*P* < 0.05 compared with WT chow. **P* < 0.05 compared with WT HF or vehicle HF. (A high-quality color representation of this figure is available in the online issue.)

include reduced collagen, increased MMP9 activity, and increased vascularization.

Genetic deletion of integrin $\alpha_2\beta_1$ diminishes skeletal muscle insulin resistance associated with HF feeding. Integrins $\alpha_1\beta_1$ and $\alpha_2\beta_1$ are collagen receptors expressed on the endothelial cell surface (19,20), as well as on several other cell types (8). To test the role of ECM-integrin signaling in the pathogenesis of insulin resistance, we assessed insulin action in chow and HF-fed *itga1*$^{-/-}$ and *itga2*$^{-/-}$ mice using insulin clamps. HF feeding increased body weight, body fat, and basal 5-h fasting glucose and insulin levels in all genotypes (Table 1). Body weights and body fat were not different between null mice and their respective WT littermates either on chow or HF diet. Basal 5-h fasting blood glucose did not differ between *itga1*$^{+/+}$ and *itga1*$^{-/-}$ mice regardless of diet; however, the basal 5-h fasting blood glucose was lower in the HF-fed *itga2*$^{-/-}$ mice compared with HF-fed *itga2*$^{+/+}$ mice. Blood glucose was maintained at 150 ~160 mg/dL during the insulin clamp in all groups (Table 1 and Fig. 4*A*, *D*, *G*, and *J*). Plasma insulin was not different between null mice and their respective WT littermates either in basal or insulin-clamped state within a specific diet (Table 1).

In chow-fed mice, GIR during the insulin clamp were not different between *itga1*$^{-/-}$ and *itga1*$^{+/+}$ mice or *itga2*$^{-/-}$ and *itga2*$^{+/+}$ mice (Fig. 4*B* and *E*). R_g in muscle was also not affected by genotype (Fig. 4*C* and *F*). HF feeding induced insulin resistance in all groups as shown that GIR and R_g were dramatically decreased by HF feeding (Fig. 4*B*, *C*, *E*, and *F* vs. 4*H*, *I*, *K*, and *L*). In contrast with chow-fed mice, GIR was lower in the HF-fed *itga1*$^{-/-}$ mice compared with HF-fed *itga1*$^{+/+}$ mice (Fig. 4*H*) but higher in the HF-fed *itga2*$^{-/-}$ mice when compared with HF-fed *itga2*$^{+/+}$ mice (Fig. 4*K*). Muscle R_g was not different between HF-fed *itga1*$^{-/-}$ and *itga1*$^{+/+}$ mice (Fig. 4*I*). However, muscle R_g was three- to fourfold higher in HF-fed *itga2*$^{-/-}$ compared with HF-fed *itga2*$^{+/+}$ (Fig. 4*L*).

Because integrins $\alpha_1\beta_1$ and $\alpha_2\beta_1$ are expressed in a cell type that is widely distributed (i.e., endothelial cells), the metabolic phenotype of HF-fed null mice is not necessarily

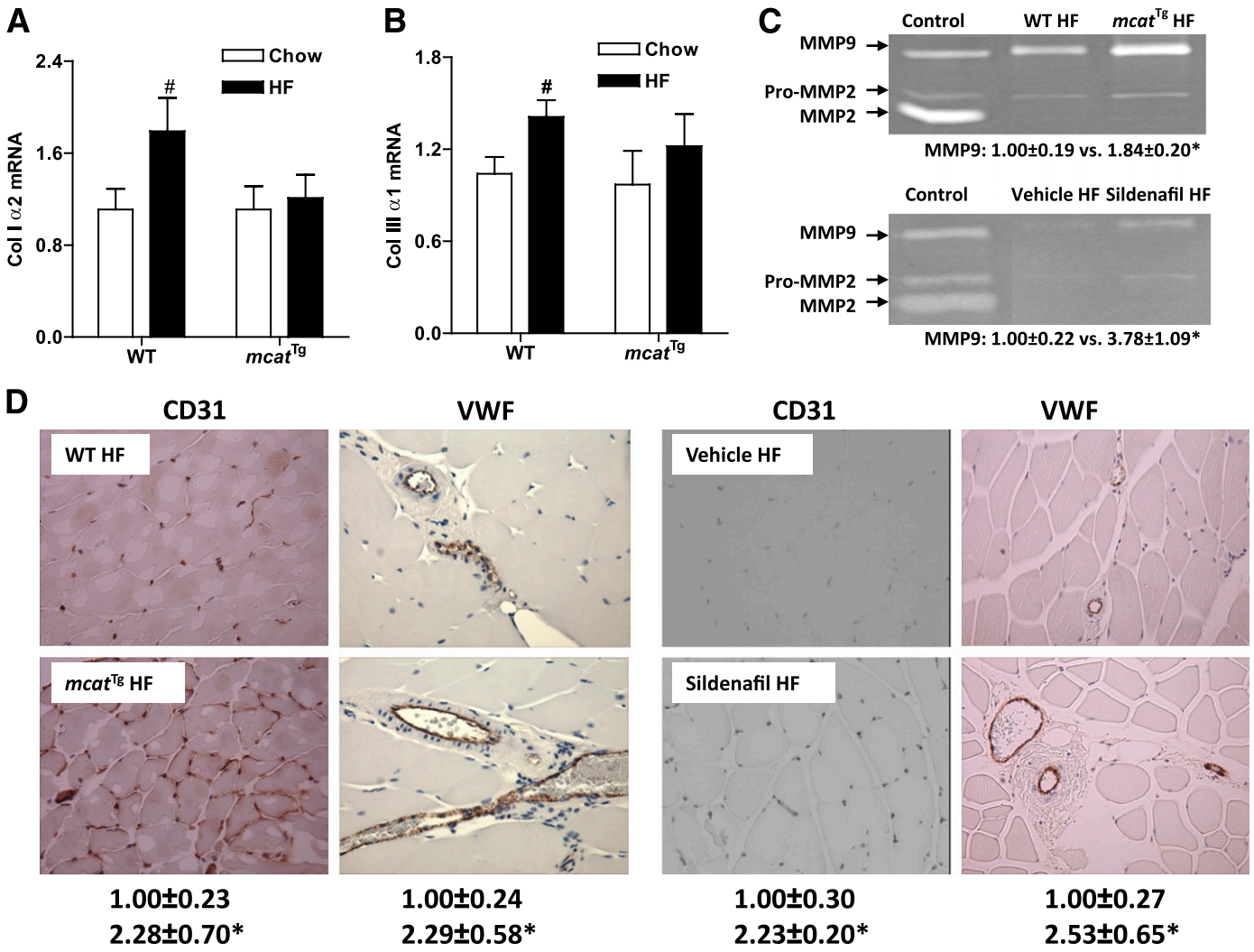

FIG. 3. Catalase overexpression and chronic treatment with sildenafil rescued muscle ECM adaptation and improved muscle vascularization. *A* and *B*: mRNA levels of ColIα2 and ColIIIα1 in gastrocnemius of WT and *mcat*^{Tg} mice. *C*: Gelatin zymogram of protein extracts from gastrocnemius of mice. MMP2 was not detectable in muscle under current experimental conditions. Arbitrary density of the MMP9 bands was listed. *D*: Immunohistochemical detection of vascular markers, CD31 and VWF. The magnification of images was 20×. Representative images are presented. Values represent means ± SE of numbers of CD31-positive structures or of areas occupied by VWF-positive structures. Data are normalized to WT HF or vehicle HF, and *n* is equal to 4 for the WT and *mcat*^{Tg} mice, 6 ~8 for the vehicle- and sildenafil-treated mice. #*P* < 0.05 compared with WT chow. **P* < 0.05 compared with WT HF or vehicle HF. (A high-quality digital representation of this figure is available in the online issue.)

restricted to muscle. Therefore, we measured insulin action in liver and adipose tissue, two other insulin-sensitive glucoregulatory organs, in HF-fed integrin null mice and WT littermates. Basal endoR_a was not different between HF-fed *itga1*$^{-/-}$ and *itga1*$^{+/+}$ mice (Fig. 5*A*). Insulin infusion decreased endoR_a by 50% in the HF-fed *itga1*$^{+/+}$ mice. In contrast, endoR_a was not suppressed in the *itga1*$^{-/-}$ mice. These data are consistent with the lower GIR and reflects greater hepatic insulin resistance in HF-fed *itga1*$^{-/-}$ mice. R_d was not different between the HF-fed *itga1*$^{-/-}$ and *itga1*$^{+/+}$ mice either in basal or insulin-clamped state (Fig. 5*B*). Insulin-stimulated adipose tissue R_g was decreased in HF-fed *itga1*$^{-/-}$ mice relative to *itga1*$^{+/+}$ mice (Fig. 5*C*). R_d was not reduced since white adipose tissue is a small contributor to total glucose disposal. EndoR_a was not different between the *itga2*$^{-/-}$ mice and the *itga2*$^{+/+}$ mice either in basal or insulin-clamped state (Fig. 5*D*); however, R_d during the insulin clamp was higher in *itga2*$^{-/-}$ compared with *itga2*$^{+/+}$ (Fig. 5*E*). This is consistent with increased R_g in muscles. Adipose tissue R_g did not differ between HF-fed *itga2*$^{-/-}$ and *itga2*$^{+/+}$ mice (Fig. 5*F*). These data suggest that the HF-fed *itga1*$^{-/-}$ mice have a further impairment in hepatic and adipose insulin resistance with no impairment in muscle insulin resistance. HF-fed *itga2*$^{-/-}$ mice have improved insulin sensitivity because of decreased muscle insulin resistance.

Changes in muscle insulin signaling after the clamp were consistent with flux measurements observed during the clamp in HF-fed *itga2*$^{-/-}$ mice. Phosphorylation of IRS-1 and Akt were increased in muscle of HF-fed *itga2*$^{-/-}$ mice compared with those of the *itga2*$^{+/+}$ littermates, indicative of improved insulin signaling (Fig. 6*A* and *B*). There was no effect on total Akt and IRS-1 in HF-fed *itga2*$^{-/-}$ mice. **Decreased skeletal muscle insulin resistance in HF-fed *itga2*$^{-/-}$ mice was associated with unchanged collagen expression and increased muscle vascularization.** In contrast with our findings in *mcat*^{Tg} and sildenafil-treated mice, the HF-fed *itga2*$^{-/-}$ mice were protected against HF-induced muscle insulin resistance despite no reduction in muscle ColIII and ColIV proteins (Fig. 6*C*).

TABLE 1
Characteristics of the integrin deficient mice

	$\alpha_1\beta_1$				$\alpha_2\beta_1$			
	Chow		HF		Chow		HF	
	itga1$^{+/+}$	*itga1*$^{-/-}$	*itga1*$^{+/+}$	*itga1*$^{-/-}$	*itga2*$^{+/+}$	*itga2*$^{-/-}$	*itga2*$^{+/+}$	*itga2*$^{-/-}$
N	7	7	5	5	5	3	6	5
Weight (g)	29 ± 1	28 ± 1	46 ± 1	45 ± 1	27 ± 1	28 ± 1	49 ± 2	48 ± 1
Body fat (%)	9 ± 1	8 ± 1	38 ± 1	41 ± 1	6 ± 1	6 ± 2	41 ± 1	40 ± 1
Age at study (weeks)	28	28	28	28	23	23	23	23
Duration on HF (weeks)	—	—	16	16	—	—	14	14
Blood glucose (mg/dL)								
Basal	129 ± 5	124 ± 2	166 ± 9	167 ± 8	137 ± 3	137 ± 1	190 ± 3	154 ± 5*
Clamp	149 ± 3	146 ± 2	153 ± 3	153 ± 2	152 ± 3	153 ± 17	156 ± 2	157 ± 4
Plasma insulin (ng/mL)								
Basal	1.5 ± 0.2	1.4 ± 0.1	7.2 ± 1.5	6.6 ± 1.1	0.7 ± 0.2	0.8 ± 0.3	9.6 ± 1.6	11.7 ± 1.2
Clamp	6.0 ± 0.6	4.6 ± 0.5	9.5 ± 0.8	8.9 ± 1.4	3.8 ± 0.7	4.6 ± 0.7	11.7 ± 1.2	14.0 ± 0.5

Data are expressed as means ± SE. *$P < 0.05$ *itga2*$^{-/-}$ HF vs. *itga2*$^{+/+}$ HF.

Nevertheless, immunostaining of the blood vessels by CD31 and VWF was increased in muscle of HF-fed *itga2*$^{-/-}$ compared with HF-fed *itga2*$^{+/+}$ mice (Fig. 6*C*). This is consistent with results obtained in *mcat*^{Tg} and sildenafil-treated mice. These data provide further evidence for the association between increased muscle insulin sensitivity and vascularization.

DISCUSSION

Our studies show that HF-fed insulin-resistant mice are characterized by an increase in muscle collagen. It is important to recognize that this is not a response that is isolated to this murine model, but is an established characteristic of human insulin resistant muscle (4,5). Thus the study of collagen and ECM in HF-fed mouse has great relevance to the human condition. By the use of genetically modified and sildenafil-treated mice, the current study demonstrates a close association between collagen dynamics and the pathogenesis of muscle insulin resistance. Furthermore, studies in *itga2*$^{-/-}$ mice provide mechanistic insight for this association by showing that the link between muscle insulin resistance and increased collagen is uncoupled in the absence of collagen-integrin $\alpha_2\beta_1$ interaction.

Inflammation can cause insulin resistance (34), and collagen deposition and ECM remodeling are hallmarks of inflammation (2). Here we tested the hypothesis that the inflammatory response associated with a HF diet would increase collagen, causing a formidable barrier to muscle glucose uptake and affecting muscle vascular reactivity (Fig. 7). In the current study, overexpression of catalase in the mitochondria, which reduces oxygen free radical production, prevented muscle inflammation, diminished collagen expansion, improved vascularity, and rescued insulin resistance. It is known that PDE5a inhibition increases vascular reactivity. PDE5a inhibition prevented collagen expansion by decreasing the inflammatory response. PDE5a inhibition, like catalase overexpression, rescued insulin resistance. Integrin $\alpha_2\beta_1$ is expressed in endothelial cells (8), and loss of integrin $\alpha_2\beta_1$ leads to increased endothelial cell proliferation and angiogeneis in vivo (20). Endothelial/vascular dysfunction is associated with insulin resistance (35). Here we found that enhanced muscle insulin action in mice lacking the integrin $\alpha_2\beta_1$ receptor was also associated with increased angiogenesis. We postulate that the lack of an adaptive increase in vascularization and endothelial function contributes to diet-induced insulin resistance in C57BL/6J mice. Murine models that are able to adapt in this way have diminished insulin resistance.

TNF-α, a cytokine involved in systemic inflammation, has been shown to regulate collagen expression (36,37). In line with decreased muscle inflammation and collagen expression, *mcat*^{Tg} mice also had decreased muscle *TNF-α* gene expression. These data suggest that inflammation increases collagen expression possibly mediated via TNF-α. Although TNF-α mRNA tended to be reduced in HF-fed sildenafil-treated mice when compared with the HF-fed control mice, differences were not significant. This suggests that factors other than TNF-α could also play a role in inflammation-mediated collagen regulation.

We showed that the increases in muscle collagen were corrected when muscle insulin resistance was rescued either by genetic manipulation (*mcat*^{Tg}) or pharmacological treatment (sildenafil). It is important to note that these two models improve muscle insulin sensitivity and suppress the diet-induced increases in ColIII and ColIV, by distinct primary mechanisms. *mcat*^{Tg} reduces mitochondrial release of ROS (21), whereas chronic treatment with sildenafil inhibits PDE5a, causing an induction of smooth muscle relaxation and vasodilation (22). Thus, despite targeting different initial pathways within skeletal muscle, both models reverse excess collagen deposition in response to HF feeding. Bajaj et al. (38) showed that a sustained reduction in plasma free fatty acids in insulin-resistant relatives of patients with type 2 diabetes leads to an increase in insulin sensitivity, but paradoxically increases mRNA for ECM proteins. Differences in the experimental paradigm make it difficult to compare those results with findings from the current study and previous studies in humans from the same laboratory (4). Whether this paradoxical increase in collagen gene expression observed in the study of Bajaj et al. is paralleled by an increase in protein was not assessed. Acipimox, a nicotinic acid analog that activates G_i protein-coupled receptors (39), was used to lower free fatty acids in the study of Bajaj et al. It is possible that acipimox affects collagen mRNAs independent of effects on insulin action. It is clear that the association between ECM remodeling, free fatty acids, and insulin resistance is complex and remains to be fully defined.

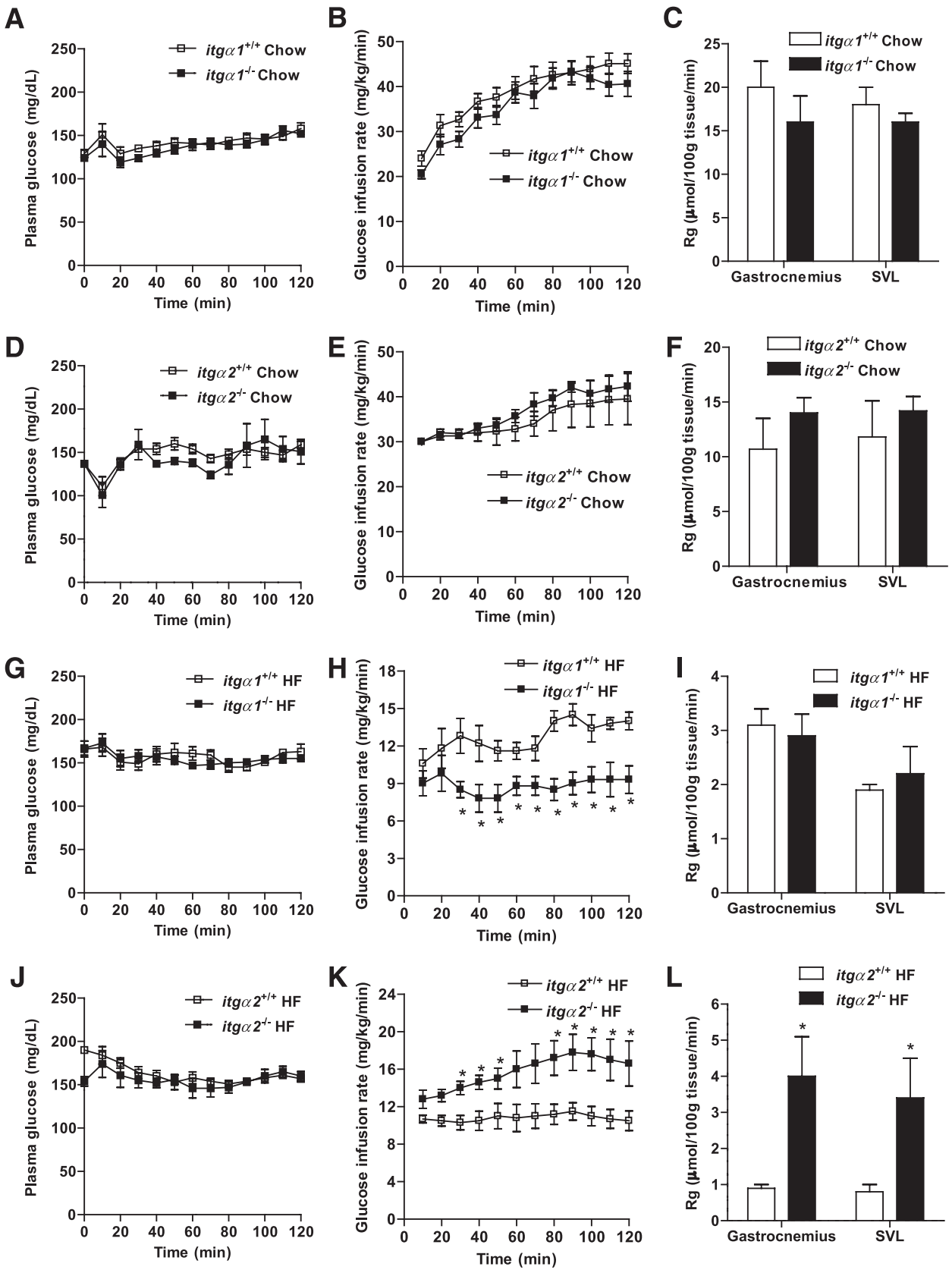

FIG. 4. Blood glucose, glucose infusion rates, and muscle glucose uptake (R_g) in the chow- and HF-fed integrin α_1- and integrin α_2-null mice during the hyperinsulinemic-euglycemic clamp. *A*, *D*, *G*, and *J*: Blood glucose was maintained at 150 ~160 mg/dL in all groups of mice. Time course is presented to illustrate the quality of the clamps. *B*, *E*, *H*, and *K*: To maintain this euglycemia, 50% glucose was infused into mice throughout the clamp. *C*, *F*, *I*, and *L*: Nonmetabolizable glucose analog [^{14}C]2-deoxyglucose was administered as an intravenous bolus to determine the glucose uptake (R_g) in muscles. Values represent means ± SE, n = 3 ~7 for each group. *$P < 0.05$ compared with *itgα1*$^{+/+}$ HF or *itgα2*$^{+/+}$ HF. SVL, superficial vastus literalis.

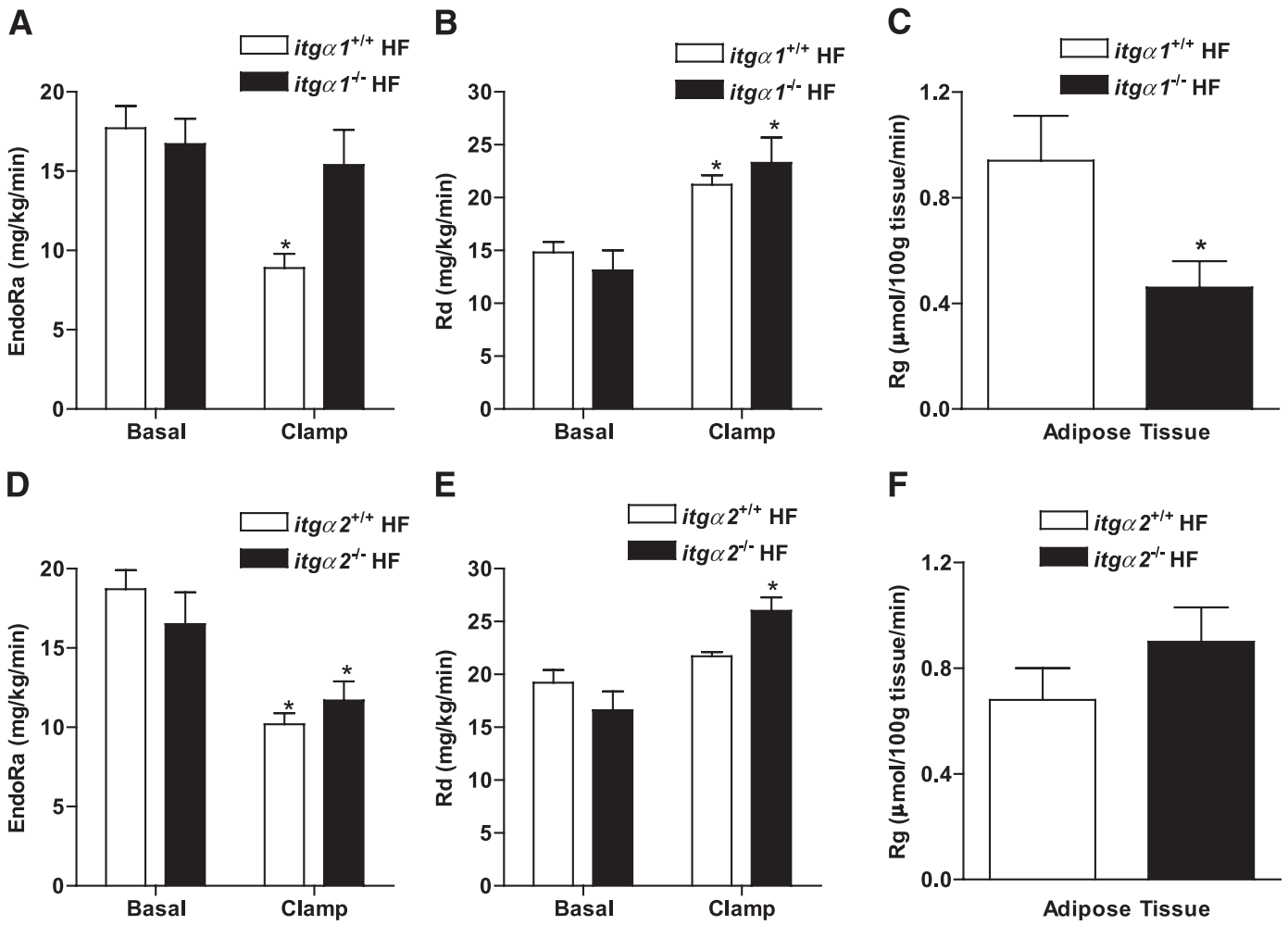

FIG. 5. Insulin sensitivity in liver and adipose tissue of HF-fed integrin α_1- and integrin α_2-null mice during the hyperinsulinemic-euglycemic clamp. *A* and *D*: Endogenous glucose production (endoR_a) was calculated by subtracting the glucose infusion rate from total R_a. *B* and *E*: Glucose disappearance rate (R_d) was determined using non-steady-state equations. *C* and *F*: Nonmetabolizable glucose analog [^{14}C]2-deoxyglucose was administered as an intravenous bolus to determine the glucose uptake (R_g) in adipose tissue. Values represent means ± SE; n = 5 ~6 for each group. For *A*, *B*, *D*, and *E*, *$P < 0.05$ compared with *itga1*$^{+/+}$ HF at basal or *itga2*$^{+/+}$ HF at basal. For *C*, *$P < 0.05$ compared with *itga1*$^{+/+}$ HF.

ECM-integrin signaling has been associated with insulin resistance (9,10). Because the two major collagen binding receptors integrin $\alpha_1\beta_1$ and $\alpha_2\beta_1$ have been implicated in inflammation (40) and angiogenesis (18,20), as well as collagen synthesis (14,16), we used mice selectively lacking integrin $\alpha_1\beta_1$ or $\alpha_2\beta_1$ to examine the role of collagen-integrin interaction in the development of insulin resistance. Consistent with our hypothesis, insulin resistance was exacerbated in HF-fed *itga1*$^{-/-}$ mice because of further impairments in hepatic and adipose insulin resistance. Muscle insulin resistance in HF-fed *itga1*$^{-/-}$ mice was not further impaired, possibly because of an already high resistance in muscle. In contrast with integrin $\alpha_1\beta_1$, deletion of integrin $\alpha_2\beta_1$ protected against muscle insulin resistance induced by HF feeding. Integrin $\alpha_2\beta_1$ is shown to be a positive regulator of collagen expression when cultured cells expressing $\alpha_2\beta_1$ grow in three-dimensional collagen gel (16,17). However, we found no changes in muscle collagen expression in HF-fed *itga2*$^{-/-}$ mice. This disparity could be because of differences in models and/or cell types studied. Conversely muscle vascularization was increased, which we hypothesize contributes to decreased HF-induced muscle insulin resistance in *itga2*$^{-/-}$ mice. This observation is consistent with the antiangiogenic nature of integrin $\alpha_2\beta_1$ (20). The fact that deletion of integrin $\alpha_2\beta_1$ improves diet-induced muscle insulin resistance without a reduction in muscle collagen suggests that ECM collagen expansion is associated with muscle insulin resistance by interaction with integrin $\alpha_2\beta_1$.

Although deletion of integrin $\alpha_2\beta_1$ improves HF-induced muscle insulin resistance, as shown by an approximate fourfold increase in R_g, muscle insulin sensitivity in the HF-fed *itga2*$^{-/-}$ mice is still below that seen in chow-fed *itga2*$^{+/+}$. This suggests that although the collagen-integrin $\alpha_2\beta_1$ interaction is an important determinant of insulin resistance it, not surprisingly, is just one piece of the insulin resistance syndrome. Deletion of the integrin β_1-subunit specifically in striated muscle results in insulin resistance in chow-fed mice (10). It is possible that α-subunits other than α_1 and α_2, which dimerize with the integrin β_1-subunit, may also contribute to insulin resistance. ColIII and ColIV protein was increased in muscle of HF-fed mice. It is also possible that the expanded collagens increase the spatial barrier and the nature of the physical barrier from blood to muscle, thus contributing to insulin resistance. In contrast with ColIII and ColIV, protein expression of ColI was very

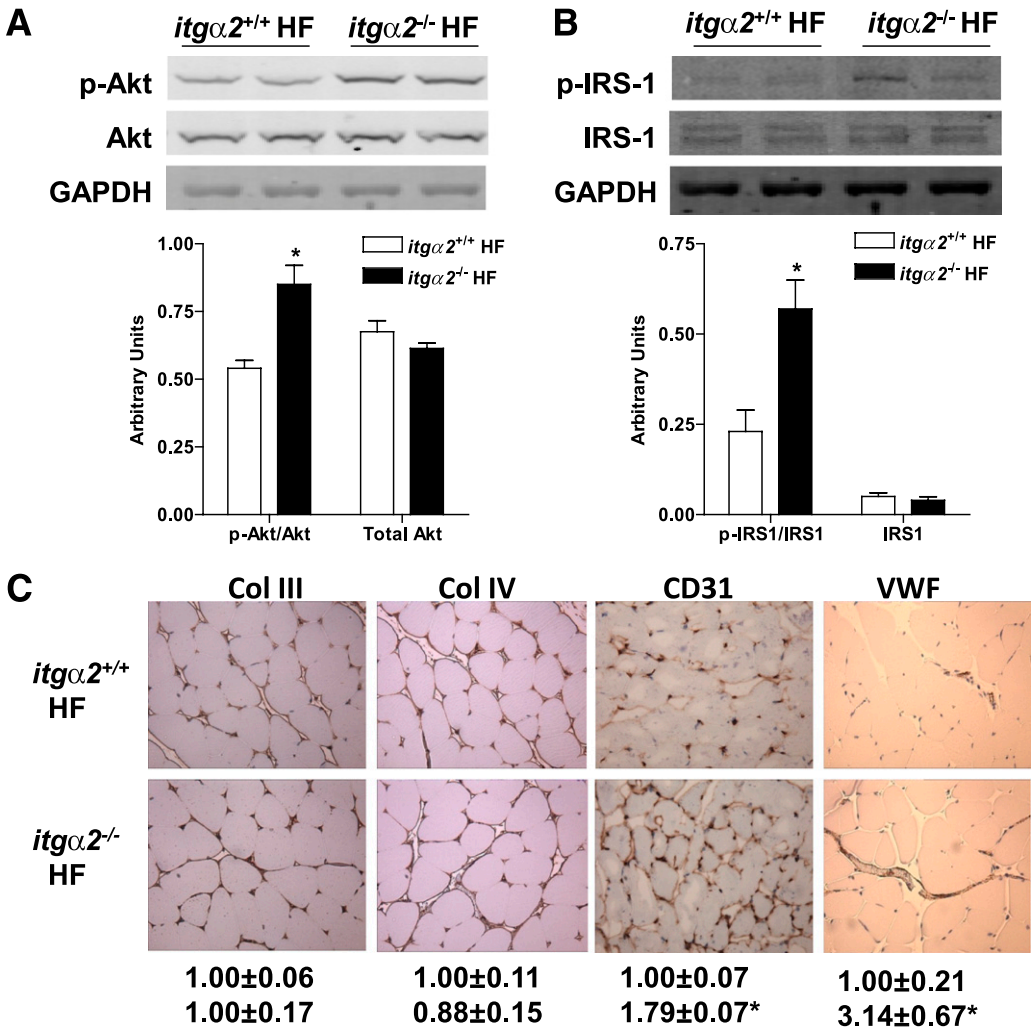

FIG. 6. Insulin signaling, collagen expression, and vascularization in gastrocnemius muscle of HF-fed *itga2*$^{+/+}$ and *itga2*$^{-/-}$ mice. *A* and *B*: Tissue homogenates extracted from gastrocnemius were applied to 4–12% SDS-PAGE gel. Western blotting was then performed using the antiphospho-Akt or antiphospho-IRS-1. Values are expressed as means ± SE of integrated intensity, and representative bands are presented; $n = 5 \sim 6$. *$P < 0.05$ compared with *itga2*$^{+/+}$ HF. *C*: Paraffin-embedded tissue sections were stained with anti-ColIII, anti-ColIV, or anti-VWF antibodies. Frozen tissue sections were stained with anti-CD31 antibody. The magnification of images was 20×. Data are expressed as means ± SE of integrated intensity of staining for ColIII and ColIV, or of numbers of CD31-positive structures, or of areas occupied with VWF-positive structures in each section. Representative images are presented; *N* is equal to 6 for the *itga2*$^{+/+}$ HF group and 3 ~6 for the *itga2*$^{-/-}$ HF group. *$P < 0.05$ *itga2*$^{-/-}$ HF vs. *itga2*$^{+/+}$ HF. (A high-quality color representation of this figure is available in the online issue.)

low in muscle, suggesting it does not create a spatial barrier. However, the mRNA levels of both ColIα1 and ColIα2 were increased in muscle of HF-fed mice, implying that ColI remodeling could also be a part of insulin resistance. The interaction between ColI and integrins even at a very low level could conceivably impact cell signaling. There is the potential for interaction between the ECM and many cell surface receptors besides integrins, such as discoidin domain and growth factor receptors (41). These interactions could produce chemical or mechanical signal transduction changes that have impact on intracellular pathways.

These data obtained in murine models extend studies conducted in human subjects, which have shown that insulin-resistant humans have increased muscle collagen (4,5). We show for the first time that distinct genetic and pharmacological murine models that correct insulin resistance prevent the accumulation of collagen in skeletal muscle and exhibit increased muscle vascularity. Through the use of *itga2*$^{-/-}$ mice we provide mechanistic insight into this association by showing that the link between muscle insulin resistance and increased collagen is uncoupled in the absence of integrin $\alpha_2\beta_1$. The deletion of integrin $\alpha_2\beta_1$ also promotes increased vascularization in muscle. The results support the concept that increased collagen contributes to insulin resistance through interaction with endothelial integrin $\alpha_2\beta_1$ protein. Therefore, our findings demonstrate novel roles of ECM expansion in the pathogenesis of insulin resistance. Manipulations that limit ECM expansion or target integrin signaling may provide new opportunities to explore therapeutics for insulin resistance and type 2 diabetes.

ACKNOWLEDGMENTS

This work was supported by National Institutes of Health Grants DK-54902 and DK-59637 (Mouse Metabolic Phenotyping Center).

No potential conflicts of interest relevant to this article were reported.

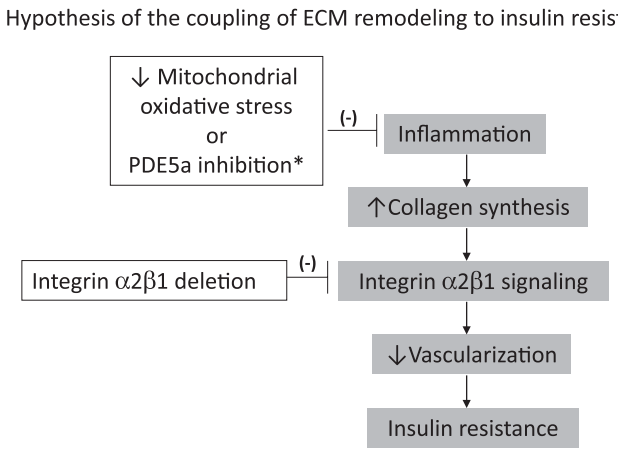

FIG. 7. Proposed model for how ECM remodeling is linked to HF diet-induced muscle insulin resistance. HF diet potentially leads to insulin resistance by several mechanisms. This scheme illustrates our hypothesis that multiple mechanisms are involved in this pathway, including inflammation, ECM expansion, integrin $\alpha_2\beta_1$ activation, and vascularization in muscle. Interruptions of the pathway at several steps rescue insulin resistance.

L.K. researched data and wrote the article. J.E.A. and R.S.L.-Y. contributed to discussion and reviewed and edited the article. Z.Z. contributed to discussion. F.D.J. researched data. P.D.N., A.P., M.M.Z., and D.H.W. contributed to discussion and reviewed and edited the article.

The authors thank Melissa B. Downing, Pamela S. Wirth, and Dr. Lillian B. Nanney of the Vanderbilt Immunohistochemistry Core Laboratory for performing the immunohistochemistry.

REFERENCES

1. Aumailley M, Gayraud B. Structure and biological activity of the extracellular matrix. J Mol Med 1998;76:253–265
2. Khoshnoodi J, Pedchenko V, Hudson BG. Mammalian collagen IV. Microsc Res Tech 2008;71:357–370
3. Yurchenco PD, Patton BL. Developmental and pathogenic mechanisms of basement membrane assembly. Curr Pharm Des 2009;15:1277–1294
4. Richardson DK, Kashyap S, Bajaj M, et al. Lipid infusion decreases the expression of nuclear encoded mitochondrial genes and increases the expression of extracellular matrix genes in human skeletal muscle. J Biol Chem 2005;280:10290–10297
5. Berria R, Wang L, Richardson DK, et al. Increased collagen content in insulin-resistant skeletal muscle. Am J Physiol Endocrinol Metab 2006;290: E560–E565
6. Hynes RO. Integrins: bidirectional, allosteric signaling machines. Cell 2002; 110:673–687
7. Askari JA, Buckley PA, Mould AP, Humphries MJ. Linking integrin conformation to function. J Cell Sci 2009;122:165–170
8. McCall-Culbreath KD, Zutter MM. Collagen receptor integrins: rising to the challenge. Curr Drug Targets 2008;9:139–149
9. Bisht B, Goel HL, Dey CS. Focal adhesion kinase regulates insulin resistance in skeletal muscle. Diabetologia 2007;50:1058–1069
10. Zong H, Bastie CC, Xu J, et al. Insulin resistance in striated muscle-specific integrin receptor beta1-deficient mice. J Biol Chem 2009;284: 4679–4688
11. Abair TD, Sundaramoorthy M, Chen D, et al. Cross-talk between integrins alpha1beta1 and alpha2beta1 in renal epithelial cells. Exp Cell Res 2008; 314:3593–3604
12. Znoyko I, Trojanowska M, Reuben A. Collagen binding alpha2beta1 and alpha1beta1 integrins play contrasting roles in regulation of Ets-1 expression in human liver myofibroblasts. Mol Cell Biochem 2006;282: 89–99
13. Chen X, Moeckel G, Morrow JD, et al. Lack of integrin alpha1beta1 leads to severe glomerulosclerosis after glomerular injury. Am J Pathol 2004;165: 617–630
14. Chen X, Abair TD, Ibanez MR, et al. Integrin alpha1beta1 controls reactive oxygen species synthesis by negatively regulating epidermal growth factor receptor-mediated Rac activation. Mol Cell Biol 2007;27:3313–3326
15. Honoré S, Kovacic H, Pichard V, Briand C, Rognoni JB. Alpha2beta1-integrin signaling by itself controls G1/S transition in a human adenocarcinoma cell line (Caco-2): implication of NADPH oxidase-dependent production of ROS. Exp Cell Res 2003;285:59–71
16. Ivaska J, Reunanen H, Westermarck J, Koivisto L, Kähäri VM, Heino J. Integrin alpha2beta1 mediates isoform-specific activation of p38 and upregulation of collagen gene transcription by a mechanism involving the alpha2 cytoplasmic tail. J Cell Biol 1999;147:401–416
17. Langholz O, Röckel D, Mauch C, et al. Collagen and collagenase gene expression in three-dimensional collagen lattices are differentially regulated by alpha 1 beta 1 and alpha 2 beta 1 integrins. J Cell Biol 1995;131: 1903–1915
18. Pozzi A, Moberg PE, Miles LA, Wagner S, Soloway P, Gardner HA. Elevated matrix metalloprotease and angiostatin levels in integrin alpha 1 knockout mice cause reduced tumor vascularization. Proc Natl Acad Sci USA 2000; 97:2202–2207
19. Abair TD, Bulus N, Borza C, Sundaramoorthy M, Zent R, Pozzi A. Functional analysis of the cytoplasmic domain of the integrin alpha1 subunit in endothelial cells. Blood 2008;112:3242–3254
20. Zhang Z, Ramirez NE, Yankeelov TE, et al. Alpha2beta1 integrin expression in the tumor microenvironment enhances tumor angiogenesis in a tumor cell-specific manner. Blood 2008;111:1980–1988
21. Anderson EJ, Lustig ME, Boyle KE, et al. Mitochondrial H2O2 emission and cellular redox state link excess fat intake to insulin resistance in both rodents and humans. J Clin Invest 2009;119:573–581
22. Ayala JE, Bracy DP, Julien BM, Rottman JN, Fueger PT, Wasserman DH. Chronic treatment with sildenafil improves energy balance and insulin action in high fat-fed conscious mice. Diabetes 2007;56:1025–1033
23. Kim J, Seok YM, Jung KJ, Park KM. Reactive oxygen species/oxidative stress contributes to progression of kidney fibrosis following transient ischemic injury in mice. Am J Physiol Renal Physiol 2009;297:F461–F470
24. Yang L, Zou XJ, Gao X, et al. Sodium tanshinone IIA sulfonate attenuates angiotensin II-induced collagen type I expression in cardiac fibroblasts in vitro. Exp Mol Med 2009;41:508–516
25. Cai J, Yi FF, Bian ZY, et al. Crocetin protects against cardiac hypertrophy by blocking MEK-ERK1/2 signalling pathway. J Cell Mol Med 2009;13:909–925
26. Park J, Ha H, Kim MS, Ahn HJ, Huh KH, Kim YS. Carvedilol inhibits platelet-derived growth factor-induced extracellular matrix synthesis by inhibiting cellular reactive oxygen species and mitogen-activated protein kinase activation. J Heart Lung Transplant 2006;25:683–689
27. Ayala JE, Bracy DP, McGuinness OP, Wasserman DH. Considerations in the design of hyperinsulinemic-euglycemic clamps in the conscious mouse. Diabetes 2006;55:390–397
28. James DE, Burleigh KM, Kraegen EW. In vivo glucose metabolism in individual tissues of the rat. Interaction between epinephrine and insulin. J Biol Chem 1986;261:6366–6374
29. Steele R, Wall JS, De Bodo RC, Altszuler N. Measurement of size and turnover rate of body glucose pool by the isotope dilution method. Am J Physiol 1956;187:15–24
30. Kraegen EW, James DE, Jenkins AB, Chisholm DJ. Dose-response curves for in vivo insulin sensitivity in individual tissues in rats. Am J Physiol 1985;248:E353–E362
31. Livak KJ, Schmittgen TD. Analysis of relative gene expression data using real-time quantitative PCR and the 2(-Delta Delta C(T)) Method. Methods 2001;25:402–408
32. Muhs BE, Gagne P, Plitas G, Shaw JP, Shamamian P. Experimental hindlimb ischemia leads to neutrophil-mediated increases in gastrocnemius MMP-2 and -9 activity: a potential mechanism for ischemia induced MMP activation. J Surg Res 2004;117:249–254
33. Collins S, Martin TL, Surwit RS, Robidoux J. Genetic vulnerability to diet-induced obesity in the C57BL/6J mouse: physiological and molecular characteristics. Physiol Behav 2004;81:243–248
34. Shoelson SE, Herrero L, Naaz A. Obesity, inflammation, and insulin resistance. Gastroenterology 2007;132:2169–2180
35. Clark MG. Impaired microvascular perfusion: a consequence of vascular dysfunction and a potential cause of insulin resistance in muscle. Am J Physiol Endocrinol Metab 2008;295:E732–E750

36. Iraburu MJ, Domínguez-Rosales JA, Fontana L, et al. Tumor necrosis factor alpha down-regulates expression of the alpha1(I) collagen gene in rat hepatic stellate cells through a p20C/EBPbeta- and C/EBPdelta-dependent mechanism. Hepatology 2000;31:1086–1093
37. Piguet PF, Collart MA, Grau GE, Sappino AP, Vassalli P. Requirement of tumour necrosis factor for development of silica-induced pulmonary fibrosis. Nature 1990;344:245–247
38. Bajaj M, Medina-Navarro R, Suraamornkul S, Meyer C, DeFronzo RA, Mandarino LJ. Paradoxical changes in muscle gene expression in insulin-resistant subjects after sustained reduction in plasma free fatty acid concentration. Diabetes 2007;56:743–752
39. Soga T, Kamohara M, Takasaki J, et al. Molecular identification of nicotinic acid receptor. Biochem Biophys Res Commun 2003;303:364–369
40. de Fougerolles AR, Sprague AG, Nickerson-Nutter CL, et al. Regulation of inflammation by collagen-binding integrins alpha1beta1 and alpha2beta1 in models of hypersensitivity and arthritis. J Clin Invest 2000;105:721–729
41. Hynes RO. The extracellular matrix: not just pretty fibrils. Science 2009; 326:1216–1219